International Journal of Microwave and Wireless Technologies

cambridge.org/mrf

Research Paper

Cite this article: Zhang J, Li H, Zheng Q, Ding J, Guo C (2018). Wideband radar cross-section reduction of a microstrip antenna using slots. *International Journal of Microwave and Wireless Technologies* **10**, 1042–1047. https://doi.org/10.1017/S1759078718000569

Received: 19 September 2017
Revised: 26 February 2018
Accepted: 1 March 2018
First published online: 7 August 2018

Key words:
Antenna design; EM field theory; modeling and measurements; radar cross-section

Author for correspondence:
Zhang JiaKai, E-mail: zjkyikun@mail.nwpu.edu.cn

Wideband radar cross-section reduction of a microstrip antenna using slots

Jiakai Zhang, Haixiong Li, Qi Zheng, Jun Ding and Chenjiang Guo

School of Electronics and Information, Northwestern Polytechnic University, Xi'an 710129, China

Abstract

In this study, a new microstrip patch antenna with wideband radar cross-section (RCS) reduction is presented. The RCS of the proposed antenna was reduced by subtracting the current-direction slots of the patch, with the radiation performance sustained not only for the current-direction subtraction, but also for the no modification in the ground plane. Modified and reference antenna were fabricated and measured. The simulation and measurement results showed that the modified antenna reduced the in-band and out-band RCS simultaneously with no detriment to the radiation performance. In the frequency band from 3.9 to 8.1 GHz, the RCS of the modified antenna was reduced in the whole band compared with the RCS of the reference antenna. The maximum RCS reduction was 7 dB at a frequency of 6.7 GHz.

Introduction

The radar cross-section (RCS) represents the detectability of an object to a radar system. With the rapid development of detection equipment, RCS reduction plays an important role in stealth technology, especially in military applications [1–3]. As a strong scattering source, the scattering performance of the antenna has a decisive influence on the total RCS of the equipment. The development of reduced RCS antenna has received high priority [4–6].

Several methods have been used to reduce the RCS of antenna and can be mainly divided into three categories. The first category is to reduce the RCS with the use of a metamaterial. The most commonly used metamaterials in the RCS reduction of antenna are with an electromagnetic band gap (EBG) [7], frequency selective surface (FSS) [8, 9], partially reflecting surface (PRS), metasurface, absorber [10], and so on [1, 11]. Reference [2] used mushroom-like EBG structures to reduce the RCS of patch antenna arrays. The antenna arrays operated in the *S*-band, whereas the RCS reduction was designed at the X-band. Kandasamy *et al.* [3] investigated a low RCS antenna based on a metasurface, where the bandwidth of the RCS reduction is restricted by the working bandwidth of the metasurface. Genovesi *et al.* [4] proposed slot antennas arrays with RCS reduction by the use of an FSS. However, the volume of the antenna increased significantly, which is a common defect of antenna RCS reduction based on metamaterials, especially with the use of an absorber [5] or PRS [6]. The second category is shaping, which involves the subtraction of part of the patch or ground plane. It is worth noting that the subtraction should be located at the weak distribution of the scattering mode. Recently, subtraction at the ground and patch planes simultaneously has been widely used, such as for octagonal-shaped antenna [12], double-sided axe-shaped antenna [13], and triangular antenna [14]. A common defect of the above antenna is the backward radiation enhanced by the subtraction of the ground plane, which is not conducive to restraining the back lobe. In addition, the effect of the shaping method in reducing the RCS and is limited in the high-frequency band [15]. The final category consists of less common methods used to reduce the RCS, such as PIN diodes [16], offset feeding [17], complementary split-ring resonators [18], and so on [19]. A characteristic of the third category is that the RCS reduction of the antenna occurs at the expense of the radiation.

The shaping method is widely used for easy fabrication and integration. Reducing the out-of-band RCS of the antenna with the use of the shaping method has been accomplished in the literature [12–14], whereas the in-band and out-of-band reduction of the RCS simultaneously is rarely accomplished. The aim of this study is to introduce an alternative shaping method to reduce the in-band and out-of-band RCS simultaneously. A new microstrip patch antenna with current-direction slots is proposed, with no modification in the ground plane. As a result, the in-band and out-band RCS of the proposed antenna are reduced simultaneously with the radiation performance sustained. Different from other shaping methods, the method in this study only modifies the patch plane. In addition, wideband RCS reduction is achieved.

Design and analysis of the reference antenna

A dielectric material with a relative dielectric constant of 2.2 is used to design the reference microstrip antenna. The size of the substrate is 27.5 mm × 27.5 mm × 2.0 mm, as shown in Fig. 1. The coordinate system and the origin are demonstrated in Fig. 1, which shows the structure of the antenna. The size of the patch is 21.6 mm × 21.6 mm. The patch and the substrate share the same central point in the coordinate system. The microstrip antenna was produced with the coaxial feed method and the coordinate of the feed point is $X_0 = 2.2$ mm and $Y_0 = 2.2$ mm. The feed point is represented as the black spot in Fig. 1.

The radiation characteristics of the reference antenna were measured using the high-frequency structure simulator, which is based on the finite element method. The return loss of the antenna is depicted in Fig. 2(a), which shows that the resonance frequency of the antenna is 4.27 GHz. Figure 2(b) demonstrates the radiation pattern of the reference antenna and it can be found that the maximum gain of the antenna is 7.06 dB. The back lobe is also shown in this figure.

The distributions of the radiating and scattering modes at the resonance frequency are exhibited in Fig. 3. It should be noted that the same color in the different images does not represent the same value. The distribution of the surface currents of the radiating mode at the resonance frequency is shown in Fig. 3(a). It is clear that the direction of the middle-area surface currents is inclined to the direction of the edge with the 45° included angle. The directions of the edge-area surface currents are parallel to the direction of the edge. The distribution of the electric field at 4.27 GHz was simulated and is shown in Fig. 3(b). It can be seen that the distribution of the electric field at 4.27 GHz is symmetrical about the diagonal of the patch, and the maximum amplitude of the electric field is located near the vertices. In the case of the scattering mode at the resonance frequency, the directions of the surface currents are parallel to the x-axis. The maximum current is located along the x-axis directional edge and the current in the middle area is larger than that in the top or bottom of the patch. Figure 3(d) shows that the maximum of the electric field is situated at the top and bottom of the patch, while the minimum is located in the middle of the patch.

In order to maintain the radiation performance, the modification of the proposed antenna should not change the surface current distribution. In this study, the direction of the surface current of the reference antenna is inclined to the direction of the edge with the 45° included angle. Therefore, the direction of the modification should be parallel to the direction of the surface current.

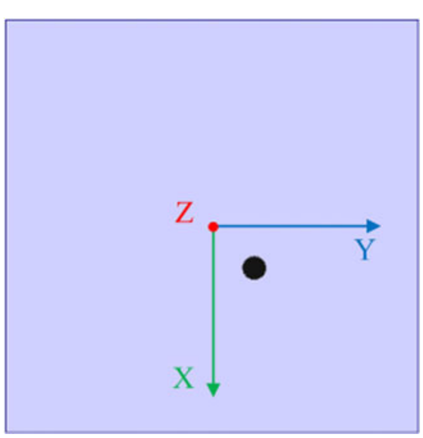

Fig. 1. Geometry of the reference antenna.

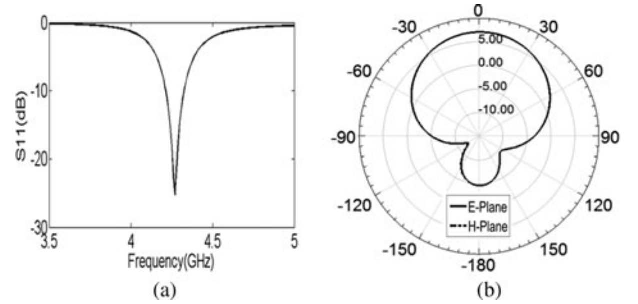

Fig. 2. Simulation results of the reference antenna. (a) Return loss, (b) radiation patterns.

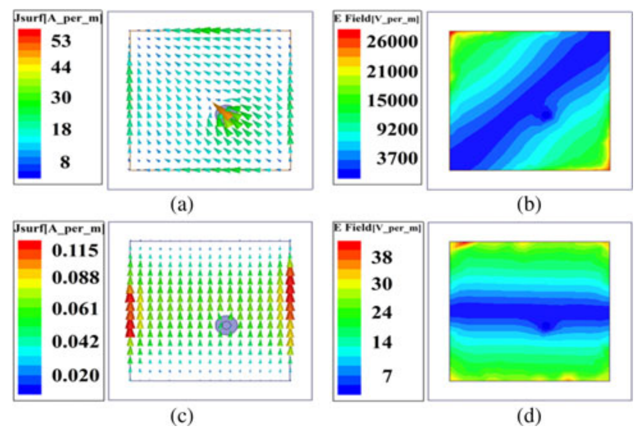

Fig. 3. Distributions of the reference antenna in the radiating and scattering modes. (a) Surface current in the radiating mode, (b) electric field in the radiating mode, (c) surface current in the scattering mode, (d) electric field in the scattering mode.

Simulation and measurement of radiation performance of the modified antenna

Antenna RCS is determined by structural mode RCS and antenna mode RCS [4], as presented in Equation (1)

$$\sigma = \left| \sqrt{\sigma_s} - (1 + \Gamma_a)\sqrt{\sigma_a} e^{j\phi} \right|^2, \quad (1)$$

where σ is the total RCS of the antenna, σ_s is the structural mode RCS, σ_a is the antenna mode RCS, Γ_a is the reflection coefficient of the antenna, and ϕ is the relative phase between the structural mode RCS and antenna mode RCS [4]. Generally, the structural mode RCS is caused by the perpendicular reflection of the antenna, and the improper impedance matching leads to the antenna mode RCS [20]. During the investigation of the antenna, the antenna is assumed to be well matched. Therefore, the RCS reduction would be obtained by reducing the structural mode RCS of the antenna.

Many factors should be taken into account for the antenna RCS reduction, such as scattering characteristics, radiation performance, the cost of the antenna, and the global performance [21]. Therefore, an elaborate design and a tradeoff has to balance the advantages against disadvantages. Furthermore, the antenna RCS reduction should be fundamental for the maintenance of

https://doi.org/10.1017/S1759078718000569 Published online by Cambridge University Press

the radiation performance. Thus, in the case of the shaping method to reduce the antenna RCS, the weak area of the patch for the distribution of the scattering field should be subtracted [22]. According to the above analysis, the proposed antenna in this paper is modified by the current-direction subtraction in the patch and without any modification to the ground plane of the antenna.

The modification was made to reduce the RCS of the reference antenna, while the radiation performance was sustained in this section. In order to maintain the radiation performance, the subtraction was introduced along the direction of the currents caused by radiation. There are nine rectangular slots subtracted from the patch, as shown in Fig. 4. The blank parts represent the slots and the part in blue refers to the patch of the antenna. The nine rectangular slots are numbered from 1 to 9 for convenient description. In addition, L_m and W_m are taken as the length variables and the width variables, respectively, in which the variable m represents the serial number of the slot. The dark plot in each slot is used to exhibit the vertices of the slots, and the coordinates of the vertices are represented as (X_m, Y_m). Thus, the location of all the slots is embodied by the coordinates of the vertices, the lengths, and the widths. The values of all the structural parameters (in mm) are listed in Table 1. The optimization process of the values is not given here for brevity. Each parameter was optimized to minimize the monostatic RCS of the modified antenna.

It should be noted that the width of each slot is limited. The large-width slot leads to an obvious edge current along the broadside of the slot, which would influence the radiation performance of the proposed antenna. In the case of the integration of two or more slots, it is the same as the case where the width of the slot is large. Therefore, in order to maintain the radiation performance of the proposed antenna, its modification consists of nine separate slots.

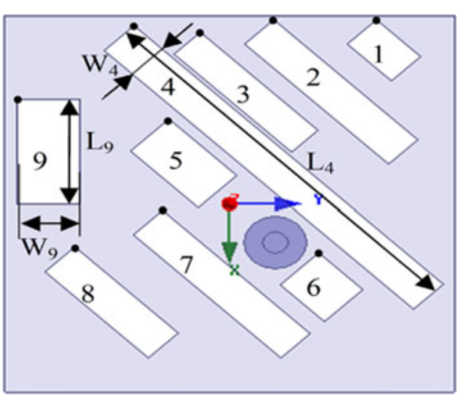

Fig. 4. Geometry of the modified antenna.

The simulation results of the proposed antenna are compared with the results of the reference antenna. Figure 5(a) shows that the resonant frequency of the proposed antenna is 4.23 GHz, as shown by the solid line. The dotted line in Fig. 5(a) represents the return loss of the reference antenna. This shows that the relative deviation of the resonant frequency is 1%, as the reference resonant frequency is 4.27 GHz. The radiation patterns of the proposed antenna are shown in Figs 5(b) and 5(c). The radiation patterns of the reference antenna and the modified antenna are compared in these figures. It can be seen that the maximum gain and the back lobe of the two antennas are almost the same.

To authenticate the results of the simulation, the prototypes of the reference and modified antenna were fabricated, as exhibited in Fig. 6. A ruler was placed close to the antenna to indicate the actual size of the prototypes, and the SMA connectors were welded in the two antennas.

The return loss of the prototypes was measured with the use of a vector network analyzer, and the measured result is presented in Fig. 7(b). The solid line shows the return loss of the modified antenna and the dotted line represents the reference antenna. By comparing the curves in Figs 7(b) and 5(a), it can be seen that the measured result agrees well with the simulated result.

Figure 7(a) shows the experimental scene of the radiation pattern measurements. The two identical horn antennas were used for the receiver and transmitter. Plastic foam with an air-like

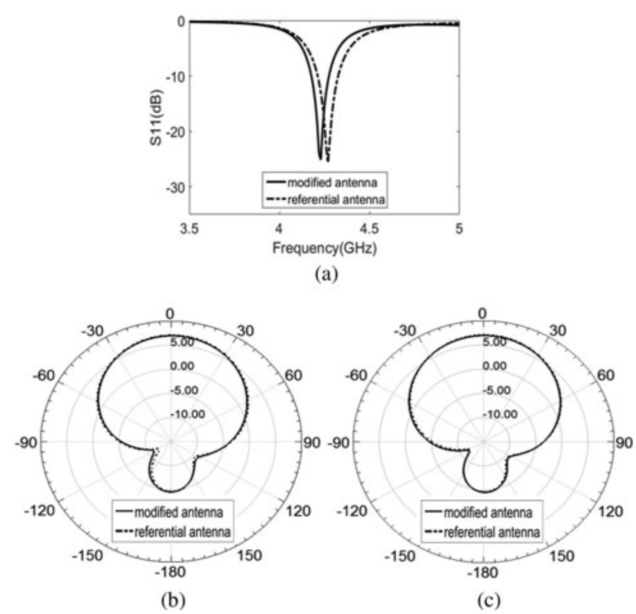

Fig. 5. Simulation results of the modified antenna. (a) Return loss, (b) radiation patterns of the E-plane, (c) radiation patterns of the H-plane.

Table 1. Parameters of the nine slots

Serial number	L_m	W_m	(X_m,Y_m)	Serial number	L_m	W_m	(X_m,Y_m)
1	3	2	(−10.6,7.1)	6	3	2.6	(2.8,4.3)
2	9.8	2	(−10.6,2.1)	7	10	2	(0.4,−3.2)
3	8	1.8	(−9.9,−1.4)	8	7	2	(2.5,−7.4)
4	21	2	(−10.3,−4.6)	9	6	3	(−6,−10.2)
5	4.6	2.6	(−4.9,−2.9)				

https://doi.org/10.1017/S1759078718000569 Published online by Cambridge University Press

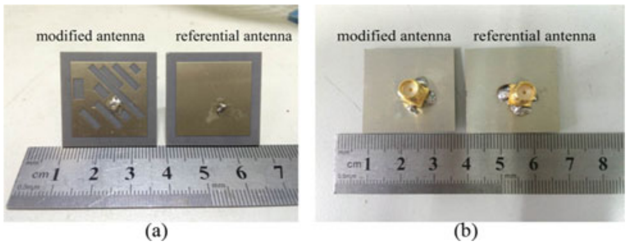

Fig. 6. Images of the two fabricated antennas. (a) Top view, (b) bottom view.

dielectric constant was used to make the center of the prototype and the center of the horn antennas at the same level.

The radiation patterns of the two antennas were measured in a microwave anechoic chamber and the resonant frequencies were chosen for 4.30 and 4.27 GHz, respectively, which were the measured resonant frequencies of the two prototype antennas. The radiation pattern results are compared in Figs 7(c) and 7(d). It can be seen that the radiation patterns of the two measured antennas are almost the same, especially for the back lobes. The slight variation between the measured and simulated results of the radiation pattern may be attributed to the welding and feed line of the excitation source. Besides, the not-perfectness of the microwave chamber is another reason of discrepancy between the simulation and measurement. Generally, the experimental and simulated results are in good agreement. This proves that the modification of the proposed antenna has no influence on the radiation performance of the reference antenna, which is the precondition of antenna RCS reduction technology.

Analysis of RCS reduction of the modified antenna

In order to further study the RCS reduction of the modified antenna, the distribution of the surface current in the radiating and scattering modes at the frequency of 4.23 GHz is investigated. The distribution of the surface current of the modified antenna in the radiating mode is shown in Fig. 8(a). One can observe that most directions of the currents are the same with the case of the reference antenna. However, the currents between slots 5 and 9, and the currents near slot 3, are slightly different from the case in Fig. 3(a). This difference causes the resonant frequency offset discussed above. The distribution of the electric field of the modified antenna is exhibited in Fig. 8(b). By comparing Figs 8(b) and 3(b), it is found that the distribution of the electric field is almost unchanged. However, it is obvious that the distribution of the surface current and the distribution of the electric field are different in scattering mode, as shown by Figs 8 and 3. From Fig. 8(c), most directions of the scattered currents are inclined to the negative direction of the x-axis, and the included angle is 45°; whereas the direction of the scattered currents of the reference antenna is parallel to the negative direction of the x-axis. As for the distribution of the scattered electric field, the distribution is similar to the distribution of the radiated electric field, whereas the amplitudes of the two figures are different.

It can be seen that the slots of the modified antenna have no influence on the current distribution in radiating mode, whereas the surface current distribution of the scattering mode has decreased and the electric field distribution has changed. Therefore, the antenna RCS reduction can be obtained by the modified antenna while the radiation performance was maintained.

Figure 9 illustrates the comparison of the monostatic RCS between the modified antenna and the reference antenna. It can

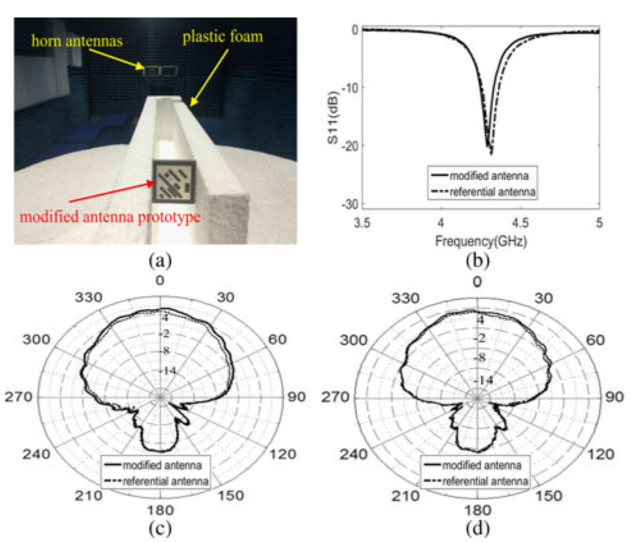

Fig. 7. Measurement and experimental results. (a) Experimental setup, (b) measured result of return loss, (c) measured result of the E-plane radiation patterns, (d) measured result of the H-plane radiation patterns.

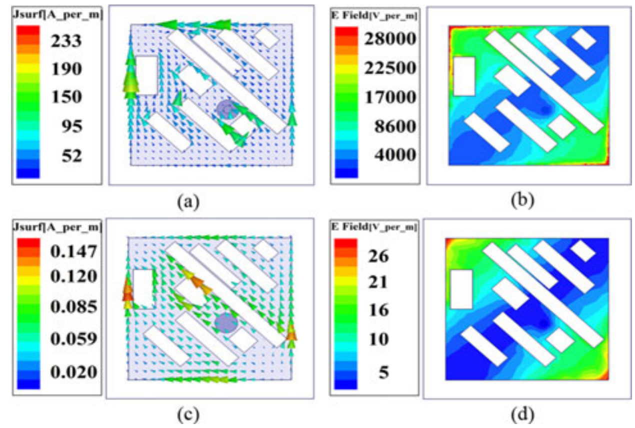

Fig. 8. Distributions of the modified antenna in the radiating and scattering modes. (a) Surface current in the radiating mode, (b) electric field in the radiating mode, (c) surface current in the scattering mode, (d) electric field in the scattering mode.

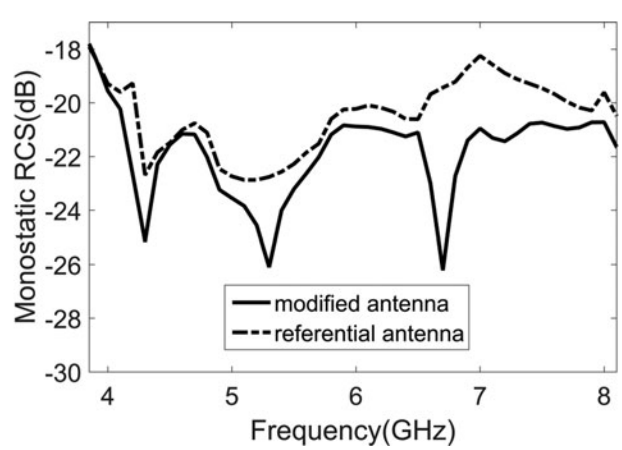

Fig. 9. Monostatic RCS of the modified and reference antenna.

https://doi.org/10.1017/S1759078718000569 Published online by Cambridge University Press

Table 2. Comparison of the antenna performance between new antenna and antennas in references

Reference	Antenna working frequency	RCS reduced frequency range	In-band or out-of-band RCS reduction	Radiation performance
[2]	3 GHz	7.5–12 GHz	Out-of-band	Maintained
[5]	3.18 GHz	3.15–3.2 GHz	In-band	Gain reduced
[6]	1.4 GHz	2–12 GHz	Out-of-band	Gain reduced
[8]	3.38 GHz	5–9.6 GHz, 10–12 GHz	Out-of-band	Gain reduced
[20]	2.5 GHz	3.8–5 GHz, 5–10 GHz	Out-of-band	Maintained
This work	1.16 GHz	1–4.4 GHz	In-band and out-of-band	Maintained

be seen that the monostatic RCS of the modified antenna dropped significantly at the frequencies of 4.3, 5.3, and 6.7 GHz, with the corresponding RCS values of −25.2, −26.1, and −26.3 dB, respectively. In addition, in the range from 3.9 to 8.1 GHz, the monostatic RCS of the whole frequency band was reduced. Therefore, the monostatic RCS of the in-band and out-band was reduced simultaneously. The maximum RCS reduction of the modified antenna is 7 dB at a frequency of 6.7 GHz. The in-band maximum RCS reduction is 2.6 dB at a frequency of 4.3 GHz.

The antenna performance of this paper is compared with other antennas proposed in the literatures, as listed in Table 2. It can be obtained that the merit of the new antenna is that the in-band and out-of-band antenna RCS can be reduced simultaneously.

Conclusions

A wideband RCS reduction microstrip patch antenna was obtained by subtracting the current-direction slots on the patch plane, with the radiation characteristics maintained. Reference and modified antennas were investigated in radiating and scattering modes, respectively. The results show that the RCS of the modified antenna is reduced from 3.9 to 8.1 GHz, and the in-band and out-band RCS reduction is achieved simultaneously. The maximum RCS reduction appears at a frequency of 6.7 GHz with a 7 dB reduction. In order to verify the analysis of the simulation, the prototypes of the two antennas were fabricated and measured. The measured results agree well with the simulated results. The modified antenna has the lower RCS in the working frequency band with the radiation performances sustained. In addition, the modification does not change the shape of the antenna or the volume of the antenna, which is pivotal to the conformal technology of the antenna. Therefore, the investigation in this study is highly meaningful for the RCS reduction technology in the antenna field.

Acknowledgement. Authors thank the reviewers and editors for their valuable comments and hard work.

References

1. **Zheng YJ, Gao J, Cao XY *et al.*** (2015) Wideband RCS reduction of a microstrip antenna using artificial magnetic conductor structures. *IEEE Antennas and Wireless Propagation Letters* **14**, 1582–1585.
2. **Panda PK and Ghosh D** (2013) Mushroom-like EBG structures for reducing RCS of patch antenna arrays, International Conference on Microwave and Photonics, Dhanbad, India.
3. **Kandasamy K, Majumder B, Mukherjee J *et al.*** (2015) Low-RCS and polarization-reconfigurable antenna using cross-slot-based metasurface. *IEEE Antennas and Wireless Propagation Letters* **14**, 1638–1641.
4. **Genovesi S, Costa F and Monorchio A** (2014) Wideband radar cross section reduction of slot antennas arrays. *IEEE Transactions on Antennas and Propagation* **62**, 163–173.
5. **Li SJ, Gao J, Cao XY *et al.*** (2015) Loading metamaterial perfect absorber method for in-band radar cross section reduction based on the surface current distribution of array antennas. *IET Microwaves, Antennas & Propagation* **9**, 399–406.
6. **Turpin JP, Sieber PE and Werner DH** (2013) Absorbing ground planes for reducing planar antenna radar cross-section based on frequency selective surfaces. *IEEE Antennas and Wireless Propagation Letters* **12**, 1456–1459.
7. **Zhang S** (2016) Novel dual-band compact HIS and its application of reducing array in-band RCS. *Microwave and Optical Technology Letters* **58**, 700–704.
8. **Zheng YJ, Gao J, Cao XY *et al.*** (2016) Wideband RCS reduction of patch array antenna with miniaturized FSS. *Microwave and Optical Technology Letters* **58**, 969–973.
9. **Shang YP, Xiao SQ and Wang BZ** (2014) Radar cross-section reduction design for a microstrip antenna. *Microwave and Optical Technology Letters* **56**, 1200–1204.
10. **Chen Q and Fu YQ** (2014) A planar stealthy antenna radome using absorptive frequency selective surface. *Microwave and Optical Technology Letters* **56**, 1788–1792.
11. **Zheng YJ, Gao J, Cao XY *et al.*** (2015) Wideband RCS reduction and gain enhancement microstrip antenna using chessboard configuration superstrate. *Microwave and Optical Technology Letters* **57**, 1738–1741.
12. **Dikmen CM, Cimen S and Cakir G** (2013) An octagonal shaped ultra wide band antenna with reduced RCS, 2nd International Japan-Egypt Conference on Electronics, Communications and Computers, Cairo, Egypt.
13. **Dikmen CM, Cimen S and Cakir G** (2013) Design of double-sided axe-shaped ultra-wideband antenna with reduced radar cross-section. *IET Microwaves, Antennas & Propagation* **8**, 571–579.
14. **Jamro DA, Hong JS, Bah MH *et al.*** (2014) Triangular antenna with novel techniques for RCS reduction applications, International Conference on Wireless Communications, Networking and Applications, Shenzen, China.
15. **Pan WB, Huang C, Chen P *et al.*** (2014) A low-RCS and high-gain partially reflecting surface antenna. *IEEE Transactions on Antennas and Propagation* **62**, 945–949.
16. **Shang Y, Xiao S, Tang MC *et al.*** (2012) Radar cross section reduction for a microstrip patch antenna using PIN diodes. *IET Microwaves, Antennas & Propagation* **6**, 670–679.
17. **Xu WW, Wang JH, Chen M *et al.*** (2014) Reduction of the in-band RCS of microstrip patch antenna by using offset feeding technique. *International Journal of Antennas and Propagation* **2014**, 303716.
18. **Liu Y, Hao YW, Jia YT *et al.*** (2014) A low RCS dual-frequency microstrip antenna with complementary split-ring resonators. *Progress in Electromagnetics Research* **146**, 125–132.
19. **Li SJ, Gao J, Cao XY *et al.*** (2014) Broadband and high-isolation dual-polarized microstrip antenna with low radar cross section. *IEEE Antennas and Wireless Propagation Letters* **13**, 1413–1416.

20. **Rajesh N, Malathi K, Raju S *et al.*** (2017) Design of vivaldi antenna with wideband radar cross section reduction. *IEEE Transactions on Antennas and Propagation* **65**, 2102–2105.
21. **Genovesi S, Costa F and Monorchio A** (2012) A low-profile array with reduced radar cross section by using hybrid frequency selective surfaces. *IEEE Transactions on Antennas and Propagation* **60**, 2327–2335.
22. **Dikmen CM, Cimen S and Cakir G** (2014) Planar octagonal-shaped UWB antenna with reduced radar cross section. *IET Microwaves, Antennas & Propagation* **62**, 2946–2953.

Zhang JiaKai was born in Shannxi Province, China, in 1990. He received the M.Sc. and B.Sc. degrees from the School of Electronics and Information, Northwestern Polytechnical University in Xi'an city, China, in 2012 and 2015, respectively. He is presently working on his doctoral degree in the School of Electronics and Information, Northwestern Polytechnical University. His research interests include electromagnetic metamaterials and antenna RCS reduction study.

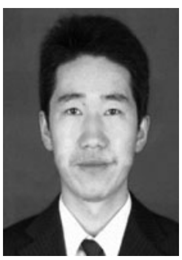

Haixiong Li was born in Shannxi Province, China, in 1982. He is an *IEEE* Student Member, *CIE* Student Member. He received the B.Sc. degree from the School of Electrical Information Science and Engineering, Lanzhou University in Lanzhou city, China, in 2006. He received the M.Sc. degree in from the School of Information Science and Technology, Xiamen University in Xiamen city, China in 2013. He is presently working on his doctoral degree in the School of Electronics and Information, Northwestern Polytechnical University in Xi'an city, China. His research interests include electromagnetic metamaterials and MIMO antenna design.

Qi Zheng was born in Anhui, China, in 1993. He received the B.S. degree in Mathematics and Applied Mathematics from the School of Science, Northwestern Polytechnical University, in Xi'an city, China, in 2014. Then, he obtained the M.S. degree in Electronic and Information Engineering from the School of Electronic and Information, Northwestern Polytechnical University, in 2016. Now, he is currently pursuing the Ph.D. degree in Electronic Science and Technology from the School of Electronic and Information, Northwestern Polytechnical University. His research interests include design of reflectarray, metamaterials, and RCS reduction.

Jun Ding was born in Shannxi Province, China, in 1964. She received the M.Sc., B.Sc., and Ph.D. degrees form the School of Electronics and Information, Northwestern Polytechnical University in Xi'an city, China, in 1986, 1989, and 2005 respectively. She is a professor in the School of Electronics and Information NWPU. She has published more than 100 research papers. Her research interests include electromagnetic metamaterials, the antenna theory and design, and the microwave circuit design.

Chenjiang Guo was born in Shannxi Province, China, in 1963. He is a CIE Senior Member, Antenna Society Committee Member. He received the M.Sc., B.Sc., and Ph.D. degrees from the School of Electronics and Information, Northwestern Polytechnical University in Xi'an city, China, in 1984, 1987, and 2007, respectively. He is a professor in the School of Electronics and Information NWPU. He has published more than 140 research papers. His research interests include EMI/EMC, the antenna theory and design, and the microwave circuit design.

https://doi.org/10.1017/S1759078718000569 Published online by Cambridge University Press